Journal of Alloys and Compounds 622 (2015) 606-609
http://dx.doi.org/10.1016/j.jallcom.2014.10.134

Analysis of magnetocaloric effect of ball milled amorphous alloys: demagnetizing factor and Curie temperature distribution

L.M. Moreno-Ramírez, J.J. Ipus, V. Franco, J.S. Blázquez, A. Conde

Dpto. Física de la Materia Condensada, ICMSE-CSIC, Universidad de Sevilla, P.O. Box 1065, 41080-Sevilla, Spain

Abstract

The magnetocaloric effect (MCE) has been measured for an amorphous mechanically alloyed (MA) $Co_{62}Nb_6Zr_2B_{30}$. It is demonstrated that sample shape must be taken into account for a correct interpretation of the results, especially to correctly determine the field dependence of magnetic entropy change and refrigerant capacity. However, although correcting the influence of the demagnetizing factor allows us to recover the theoretically predicted behavior for these field dependencies, they differ from those obtained for a rapidly quenched (RQ) amorphous alloy of the same composition. This deviation is assigned to a broader Curie temperature distribution in MA alloys with respect to RQ alloys. Theoretical simulations based on the Arrott-Noakes equation of state and a Gaussian distribution of T_C support this hypothesis.

Journal of Alloys and Compounds 622 (2015) 606-609
http://dx.doi.org/10.1016/j.jallcom.2014.10.134

1. Introduction

The magnetocaloric effect (MCE) is the reversible thermal response of a material due to a change of applied magnetic field. The physical principles of this effect were established in 1918 by Weiss and Picard [1], although the first application of this effect was delayed to 1933, when W. F. Giauque achieved ultra-low temperatures (<1 K) using paramagnetic salts [2]. Nowadays, the MCE has a growing interest due to its possible use in room temperature refrigeration technology [3] , particularly after the works of Pecharsky and Gschneidner in 1997 reporting giant magnetocaloric response at room temperature for $Gd_5Si_2Ge_2$ compounds [4].

The magnetocaloric effect can be quantified as the magnetic entropy change in an isothermal process (ΔS_M) or as the temperature change in an adiabatic process (ΔT_{ad}) due to the variation of a magnetic field. The magnetic entropy change can be indirectly calculated from the magnetization data as a function of temperature and magnetic field, $M(T,H)$, using the Maxwell's relation:

$$\Delta S_M(T,H) = \mu_0 \int_0^H \left(\frac{\partial M(T,H')}{\partial T} \right)_{H'} \mathrm{d}H' \qquad (1)$$

where the initial magnetic field is assumed to be zero. Maximum values of $|\Delta S_M|$ are obtained around the temperatures of phase transitions which imply a significant change of magnetization. In materials with first order phase transition, magnetization changes abruptly leading to a large MCE response in a small temperature range (a paradigmatic example is $Gd_5Si_2Ge_2$ [4]). For materials with a second order phase transition, characterize by a continuos change of magnetization, a lower MCE response is obtained in a broader temperature range (a paradigmatic example is pure Gd [5]). In this context, soft ferromagnetic amorphous alloys show the advantages of negligible magnetic and

Journal of Alloys and Compounds 622 (2015) 606-609
http://dx.doi.org/10.1016/j.jallcom.2014.10.134
thermal hysteresis, easy tunable Curie temperature (T_C), corrosion resistance and can be produced at a low cost [6,7].

Rapid quenching (RQ) techniques have been generally used to produce amorphous alloys [8], but mechanical alloying (MA) has been also shown as an effective alternative to produce these systems [9], including soft magnetic amorphous/nanocrystalline alloys [10]. However, amorphous samples with the same composition obtained by these two techniques can show differences in macroscopic and microscopic structures that affect MCE. Concerning the macroscopic structure, one example is the sample geometry, which is particularly important for magnetic measurements. While MA leads to powder samples, RQ techniques produce ribbons or wires with a thickness of few tens of microns. In order to make magnetic measurements, whereas a thin ribbon can be aligned with the applied field contained in its plane in order to present a negligible demagnetizing factor (N~0), this is not possible for powder samples, for which the effect of demagnetizing field is unavoidable [11]. Moreover, concerning microstructure there is a higher content of inhomogeneities and structural defects in the amorphous alloys produced by MA when compared to those produced by RQ. This can lead to a broader Curie temperature distribution in the former case [12].

In this work, the effects of the demagnetizing factor and a Curie temperature distribution on a cobalt-based amorphous alloy obtained by mechanical alloying have been studied, making a comparative study with the same alloy composition produced by rapid quenching.

2. Experimental

An amorphous alloy of nominal composition $Co_{62}Nb_6Zr_2B_{30}$ was prepared from a starting mixture of elemental powders by mechanical alloying for 40 h at 350 rpm (further

Journal of Alloys and Compounds 622 (2015) 606-609
http://dx.doi.org/10.1016/j.jallcom.2014.10.134
milling parameters can be found elsewhere [13]). The alloy phase structure was characterized by X-ray diffraction (XRD) analysis. The XRD spectrum showed an amorphous phase structure of about 95%. Morphology and composition of powder samples were studied by scanning electron microscopy (SEM). SEM images in secondary electron (SE) mode show a homogeneous size distribution of spheroidal powder particles. From backscattered electrons (BSE) mode images, the presence of boron inclusions was observed [13]. The RQ sample was produced in amorphous state by melt spinning technique. Figure 1 shows the XRD patterns of both RQ and MA samples and the SE and BSE images of the MA sample.

Isothermal magnetization curves measured in the first quadrant from 0 up to an applied magnetic field of 1.5 T were obtained in a LakeShore 7407 vibrating sample magnetometer (VSM). Magnetic entropy change has been obtained using equation (1). The field dependence of the magnetic entropy change (ΔS_M) in materials with a second order phase transition can be described using a power law equation of the form $\Delta S_M=\alpha H^n$. Theoretically, the exponent n for a single phase ferromagnetic material is field independent in three temperature ranges: well below T_c (where n=1), at $T=T_c$ (where n is related to the critical exponents δ and β, n^{peak}=1+1/δ(1-1/β)) and well above T_c (where n=2) [14]. Exponent n can be calculated locally (as a function of T and H) from ΔS_M curves using:

$$n = \frac{\mathrm{d}\log(|\Delta S_M|)}{\mathrm{d}\log(H)} \tag{2}$$

Other important parameter to quantify the MCE response of the material is the refrigerant capacity (*RC*) that can be defined as the full width at half maximum (FWHM) temperature times ΔS_M at the peak temperature (ΔS_M^{peak}). Theoretically, the field dependence of *RC* can also be expressed as a power law of the form $RC=\beta H^m$ where the

Journal of Alloys and Compounds 622 (2015) 606-609
http://dx.doi.org/10.1016/j.jallcom.2014.10.134
exponent m is related to the critical exponents (m=1+1/δ). It is worth mentioning that m should be field independent [15].

3. Results and discussion

Figure 2 shows, as solid symbols, the experimentally determined ΔS_M and exponent n as a function of temperature for two values of the applied magnetic field change (ΔH=0.5 and 1 T) for the RQ and MA samples. A clear difference in T_C between RQ and MA samples is observed and it is due to the better homogenization of boron in RQ sample [11]. Results obtained without correcting the demagnetizing field for MA sample show a significant dependence of $n(T)$ with the applied magnetic field, especially for $T<<T_c$ and $T=T_c$, which is in contrast with the theoretical predictions when the internal field is used. For RQ sample, for which N~0, these abnormal dependences are not observed (figure 5).

In order to explain this anomalous behavior, we have taken into account the effect of the demagnetizing factor N=1/3 for MA sample (assuming loosely packed spherical particles) on the magnetic data. That is, to correct the data, equation (1) must be recalculated using the internal field ($H=H_{ap}-NM$) instead of the applied field H_{ap}. This correction does not significantly affect $\Delta S_M(T)$ curves (~5% reduction in magnitude) but it eliminates the field dependence of n well below T_c and at T_c, recovering the field independency predicted by the theory.

Concerning *RC* behavior, figure 3 shows the field dependence of the exponent m calculated for the RQ and MA samples. A strong field dependence of m can be observed for the MA sample using uncorrected data, which is again against theoretical predictions. However, this artificial field dependence is also corrected (as it occurs for ΔS_M at T_C) if a demagnetizing factor N=1/3 is taken into account, recovering the theoretical prediction

Journal of Alloys and Compounds 622 (2015) 606-609
http://dx.doi.org/10.1016/j.jallcom.2014.10.134
for *m* being field independent, as previously mentioned. Deviations (<5%) from the field independency can be due slight departures from N=1/3 and N=0 of the actual demagnetizing factor.

However, after taking into account the demagnetizing factor, the values of n^{peak} are clearly higher than those found for RQ alloy with the same nominal composition (n^{peak}=0.89 and 0.74 for MA and RQ samples, respectively). Moreover, *m* values are lower (m=1.05 and 1.15 for MA and RQ samples, respectively). Therefore, unrealistic critical exponents would be determined from the experimental values of *m* and *n* of the MA sample [15]. Additionally, if the $\Delta S_M(T)$ curves of the MA powder alloys are compared to those of RQ ribbons, a reduction of the peak value (ΔS_M^{peak}) as well as an increase of FWHM can be observed. As it was previously noted, the MA powder alloy contains boron inclusions [11]. This inhomogeneous B distribution can lead to the existence of a broader T_C distribution in the amorphous phase of the MA sample with respect to that of the RQ sample. Particularly, for CoB amorphous alloys, T_C is very sensitive to oscillations in B content, decreasing 30 K per at. % B [16].

To take into account the effect of a broad T_C distribution over $\Delta S_M(T)$ for the MA sample, we have used a sum of ideal $\Delta S_M(T)$ curves with a Gaussian distribution of T_C. Therefore, the total $\Delta S_M(T)$ for the MA sample can be expressed as:

$$\Delta S_M(T) = C\sum_{T_C-\Delta}^{T_C+\Delta} \Delta S_M^{ideal}(T, T_C^{'}) \exp(-(T_C - T_C^{'})^2 / 2\sigma^2) \quad (3)$$

where σ is the standard deviation of the Curie temperature distribution, 2Δ is the range of the distribution and C is a normalization constant. To obtain the ideal curves, we used the Arrott-Noakes equation of state [17]:

$$H^{1/\gamma} = a(T - T_C)M^{1/\gamma} + bM^{1/\gamma+1/\beta} \quad (4)$$

Journal of Alloys and Compounds 622 (2015) 606-609
http://dx.doi.org/10.1016/j.jallcom.2014.10.134
with critical exponents $\beta = 0.415(1)$ and $\gamma = 1.50(1)$ derived after applying the Kouvel-Fisher method (figure 4) to the RQ sample of the same nominal composition. The values of a=2.32(1) $Oe^{1/\gamma}(emu/g)^{-1/\gamma}K^{-1}$ and b=0.0635(3) $Oe^{1/\gamma}(emu/g)^{-1/\gamma-1/\beta}$ were obtained following the 3D-fitting proposed in [18]. For the RQ sample we assume that the T_C distribution is negligible. This fact is supported by the good fitting of the experimental data using the Arrott-Noakes equation of state, as it is observed in the inset of figure 4. Differences in boron content lead to a significant variation of T_C for the RQ and MA samples, as observed in figure 2. Therefore, in order to compare the different sample data, the temperature scale has been redefined as T-T_C.

The exponent n characterizing the field dependence of the simulated $\Delta S_M(T)$ curves with a T_C distribution has been obtained using equation (2) for different standard deviation of the Gaussian distributions generated using equation (3). It is worth mentioning some details about our simulations. For amorphous alloys with a Curie temperature close to room temperature, it has been shown that the Arrott-Noakes equation of state can be used to accurately fit the experimental data for a temperature range of about a hundred Kelvins around the T_C [18]. However, a theoretical Gaussian distribution is extended to infinity, which would force to use Arrott-Noakes beyond its validity range. This has been solved, in our case, by limiting the Gaussian range to Δ=150 K. Therefore, extreme contributions must be negligible in order to minimize the effect of a finite Gaussian range, which limits the σ range that can be explored. We studied the dependence of the simulated exponent n^{peak} as a function of σ for different Δ values and we found that, for $\sigma > \Delta/2.5$, n^{peak} artificially saturates deviating from the common $n^{peak}(\sigma)$ curve. Therefore, the reliable simulated values of n^{peak} are limited in our case to $\sigma \leq 60$ K (inset of figure 5). Additionally, to simulate equation (3), we have selected a T_C' step small enough to obtain results that are independent of this parameter.

Journal of Alloys and Compounds 622 (2015) 606-609
http://dx.doi.org/10.1016/j.jallcom.2014.10.134

In inset of figure 5, an increase of the exponent n^{peak} with the increase of the standard deviation can be observed. From this plot, the exponent n^{peak} of the MA sample leads to a maximum value of σ~60 K. However, as the resolution in the determination of T_{peak} has been 5K, that might imply a measured value of n^{peak} larger than the actual one [19], leading to an overestimation of σ. In fact, figure 5 shows experimental and simulated $n(T)$ curves for the MA and RQ samples using, in the case of simulated curves of the MA sample, a Gaussian Curie temperature distribution with σ=30 K, which exhibits the best agreement among our analysis. This value of σ can be related with a variation of B content of approximately 1 at. %. Moreover, the simulated curves reproduce fairly well both observed increase in n^{peak} and flattening of $n(T)$ curve for the MA sample with respect to the RQ sample. Additionally, it is also reproduced that the minimum of $n(T)$ shifts to temperatures below the mean value of T_C when a distribution of T_C exists.

4. Conclusions

The MCE response of a Co-based amorphous alloy obtained by mechanical alloying has been studied and its different behavior with respect to an amorphous system obtained by rapid quenching has been ascribed to the effects of the demagnetizing factor and the existence of a T_C distribution. Several conclusions can be derived from this study.

- MCE response of the MA sample is smaller but more extended than that of the RQ alloy.
- The demagnetizing factor does not significantly affect the magnitude of the $\Delta S_M(T)$ curves, but it must be considered for a correct interpretation of the field dependence of MCE well below T_C and at T_C. Additionally, the field dependence of *RC* is also corrected considering the demagnetizing factor.

Journal of Alloys and Compounds 622 (2015) 606-609
http://dx.doi.org/10.1016/j.jallcom.2014.10.134

- After corrections of the internal field, the value of the exponent n at T_{peak} for the MA sample is higher than that for the RQ sample.
- Inhomogeneities in B content in the amorphous matrix developed by MA may lead to the existence of a non negligible T_C distribution.
- Simulations using the Arrott-Noakes equation of state can explain the values of $n(T)$ for MA alloys. A Curie temperature distribution around 30 K is estimated, which implies a variation of 1 at. % in the B content of the matrix.
- Simulated and experimental data shows a displacement of the temperature of n^{peak} below the mean value of T_C when a distribution of Curie temperatures exists.

Journal of Alloys and Compounds 622 (2015) 606-609
http://dx.doi.org/10.1016/j.jallcom.2014.10.134

Acknowledgements

Work supported by MINECO and EU FEDER (project MAT2013-45165-P), and the PAI of the Regional Government of Andalucía (RGA) (project P10-FQM-6462).

Journal of Alloys and Compounds 622 (2015) 606-609
http://dx.doi.org/10.1016/j.jallcom.2014.10.134

Figure captions

Fig 1: SE image showing the spheroidal shape of powder particles (left upper panel), BSE image showing B inclusion as dark spots (right upper panel) of the $Co_{62}Nb_6Zr_2B_{30}$ MA alloy and XRD patterns (lower panel) of the MA and RQ alloys.

Fig 2: Experimental $\Delta S_M(T)$ and $n(T)$ curves of the $Co_{62}Nb_6Zr_2B_{30}$ RQ and MA samples for 0.5, 1.0 T of applied field (uncorrected curves, solids symbols) or internal field (corrected curves using N=1/3, hollow symbols).

Fig 3: Experimental $m(H)$ curves of the $Co_{62}Nb_6Zr_2B_{30}$ RQ and MA samples (uncorrected curve, solids symbols, and corrected curve using N=1/3, hollow symbols).

Fig 4: Kouvel-Fisher plot to obtain the critical exponents of the RQ sample. Inset: experimental and simulated curves of the magnetic entropy change (ΔH=1.5 T) using the Arrott-Noakes equation of state.

Fig 5: Experimental and simulated $n(T)$ curves for the MA and RQ samples. Inset: dependence of n^{peak} with σ of the simulated Gaussian distribution of Curie temperatures.

Journal of Alloys and Compounds 622 (2015) 606-609
http://dx.doi.org/10.1016/j.jallcom.2014.10.134

Figure 1

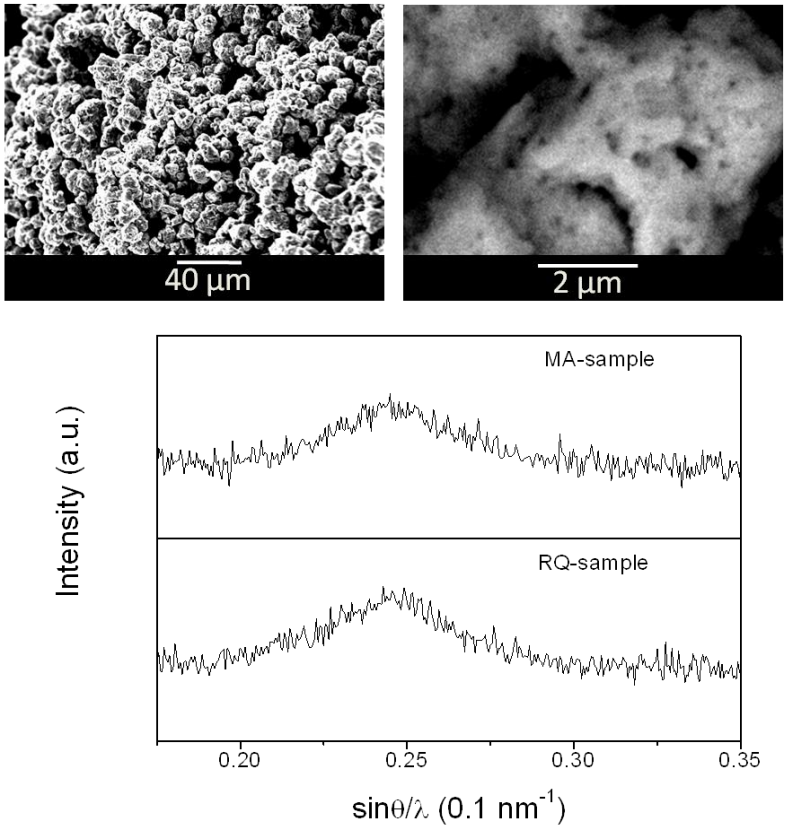

Journal of Alloys and Compounds 622 (2015) 606-609
http://dx.doi.org/10.1016/j.jallcom.2014.10.134

Figure 2

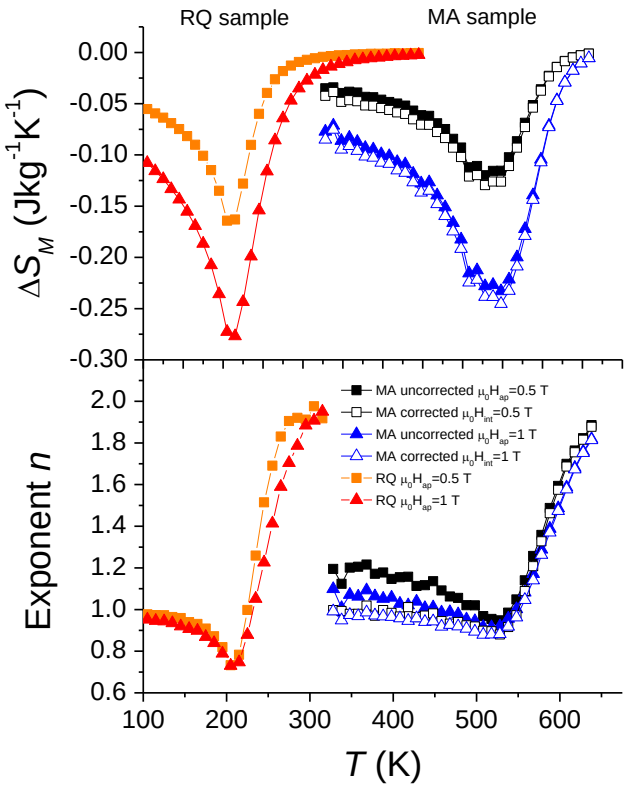

Journal of Alloys and Compounds 622 (2015) 606-609
http://dx.doi.org/10.1016/j.jallcom.2014.10.134

Figure 3

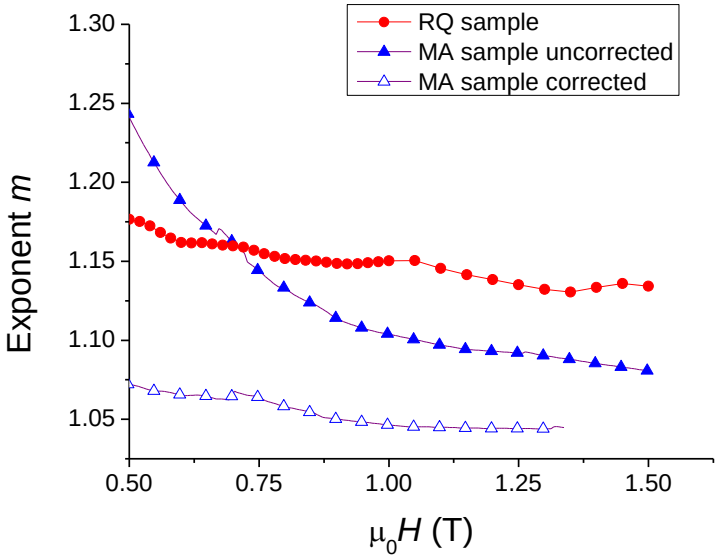

Journal of Alloys and Compounds 622 (2015) 606-609
http://dx.doi.org/10.1016/j.jallcom.2014.10.134

Figure 4

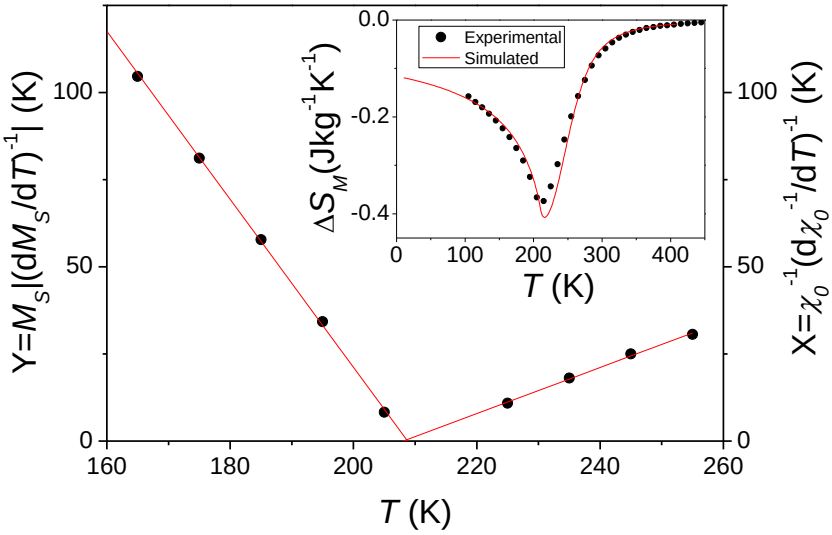

Journal of Alloys and Compounds 622 (2015) 606-609
http://dx.doi.org/10.1016/j.jallcom.2014.10.134

Figure 5

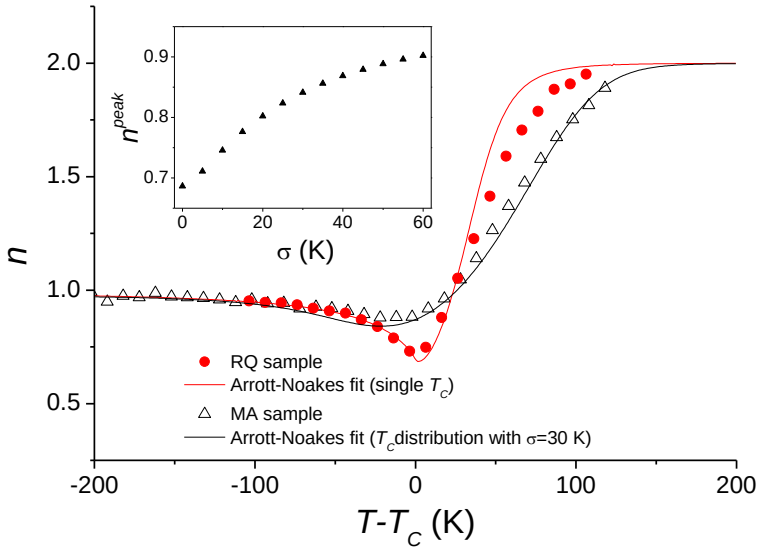

Journal of Alloys and Compounds 622 (2015) 606-609
http://dx.doi.org/10.1016/j.jallcom.2014.10.134

References

[1] P.Weiss, A. Piccard. C.R. Hebd. Séan. Acad. Sci. Paris 166 (1918) 352.
[2] W.F. Giauque, D.P. MacDougall. Phys. Rev. 43 (1933) 768.
[3] V. Franco, J.S. Blazquez, B. Ingale, A. Conde. Annu. Rev. Mater. Res. 42 (2012) 305-342.
[4] V.K. Pecharsky, K.A. Gschneidner. Phys. Rev. Lett. 78 (1997) 4494–4497.
[5] K.A. Gschneidner, V.K. Pecharsky. Annu. Rev. Mater. Sci. 30 (2000) 387–429.
[6] V. Franco, J.S. Blázquez, C.F. Conde, A. Conde. Appl. Phys. Lett. 88 (2006) 042505:1-3.
[7] V. Franco, J.S. Blázquez, M. Millán, J.M. Borrego, C.F. Conde, A. Conde. J. Appl. Phys. 101 (2007) 09C503:1-3.
[8] M. E. McHenry, M.A. Willard, D.E. Laughlin. Prog. Mater. Sci. 44 (1999) 291-433.
[9] C. Suryanarayana. Prog. Mater. Sci. 46 (2001) 1-184.
[10] J. S. Blazquez, J.J. Ipus, A. Conde, S. Lozano-Perez. JOM 65 (2013) 870-882.
[11] L.M. Moreno, J.S. Blazquez, J. J. Ipus, J. M. Borrego, V. Franco, A. Conde. J. Appl. Phys. 115 (2014) 17A302:1-3.
[12] P. Alvarez-Alonso, J.L. Sanchez Llamazares, C.F. Sanchez-Valdes, G.J. Cuello, V. Franco, P. Gorria, J.A. Blanco. J. Appl. Phys. 115 (2014) 17A929:1-3.
[13] L.M. Moreno, J.S. Blazquez, J. J. Ipus, A. Conde, J. All. Compd. 585 (2014) 485-490.
[14] V. Franco, J. S. Blazquez, and A. Conde. Appl. Phys. Lett. 89 (2006) 222512:1-3.
[15] V. Franco, A. Conde. Int. J. Ref. 33 (2010) 465-473.
[16] H. P. J. Wijn, Landolt-Börnstein Neue serie: Magnetische Eigenschaften von Metallen (Springer-Verlag, Berlin-Heidelberg, 1991), Vol. 19, p. 126.
[17] A. Arrott, J. E. Noakes, Phys. Rev. Lett. 19 (1967) 786-789.
[18] V. Franco, A. Conde, L.F. Kiss. J. Appl. Phys. 104 (2008) 033903:1-5.
[19] V. Franco, R. Caballero-Flores, A. Conde, K. E. Knipling, M. A. Willard
J. Appl. Phys. 109 (2011) 07A905:1-3.